Comparative Hybrid Life Cycle Assessment and Life Cycle Costing for the production of Steel Alloys for Recourse Efficiency

Lucy Smith[a, b], Junheng Gao[a]

[a] Department of Materials Science and Engineering, The University of Sheffield, Sheffield S1 3JD, UK

[b] Advanced Resource Efficiency Centre, The University of Sheffield, Sheffield, S10 1FL, UK

Abstract

Work to produce lightweight steel for use in the automotive industry is ongoing and through the utilisation of the material's twinning induced plasticity, light weight, high strength and ductile steel compositions have been produced. Through the application of the hybrid life cycle assessment (LCA) methodology, the aim of this study is to determine the environmental impacts of three light weight steel compositions for use in the automotive industry. The system boundary applies a cradle to gate approach against a functional unit of the production of 1kg of steel. The results show that the use of iron in each structure leads to the highest overall environmental but the use of manganese is a hotspot within the supply chain the wt% of each material type is taken into account. The addition of copper to the original steel composition has been found to reduce the global warming potential of the material structure, but increase its toxicological footprint; this must be taken into account in the decision making process to ensure that the overall impact on the environment is not increased. Finally, the major carbon hot-spot within the supply chain is the electrical energy requirements of the manufacturing process, therefore to reduce the total environmental impact of the material, efforts should be concentrated on this input.

1. Introduction

A reduction in material use, transport costs and CO_2 emissions can be achieved through the use of high strength steels in road vehicles [1]. Material development, especially in steels, has been hampered by the trade-off between strength and ductility [2] and light weight road vehicles require higher strength steels with improved damage and fracture resistance [1]. Through the exploitation of steel's twinning induced plasticity [3], strength can be enhanced without a reduction in the material's ductility [1]. This work aims to compare the environmental impact of three competing steel compositions to determine their environmental and cost impacts, thereby aiding industrial decision making for product development.

Although the substitution of one material for another might lead to a reduction of the impact of the use phase of a product (e.g. light weighting to reduce fuel usage in cars), consequently leading to savings over the whole life cycle of the product, it is necessary to determine how the composition of the material impacts the environment [4]. This study examines the comparison of three steel compositions with respect to their environmental and cost impacts. The hybrid life cycle assessment (LCA) and life cycle costing (LCC) methodologies, based on the functional unit of 1kg of steel from cradle to gate, are outlined and the results presented. Component level analysis, the manufacturing energy requirements, toxicological footprints and upstream emissions impacts are also provided and discussed within the analysis.

This report is structured as follows: the LCA and LCC methodologies are discussed in section 1; section 2 details the results; the results are then analysed in section 3; the limitations of the study are highlighted in section 4 and finally the conclusions of the report are detailed in section 5. Supplementary material is available in the Appendix.

2. Methodology

ISO 14040:2006 outlines the four standard steps (shown in Figure 1) required for the completion of a LCA; a mature methodology that aims to quantify the environmental impact of a product or service and has been widely published in many fields [5]. Figure 2 depicts the system boundary of this work and represents the 'goal and scope definition' step of the LCA, this established to represent the product or service which is to be measured [4, 6].

The Life Cycle Inventory (LCI) for this study was collected according to the production of 1kg of each alloy composition in a laboratory environment. In each case the production method described is the same (cold rolling followed by homogenisation and recrystallisation), only the alloy composition is changed.

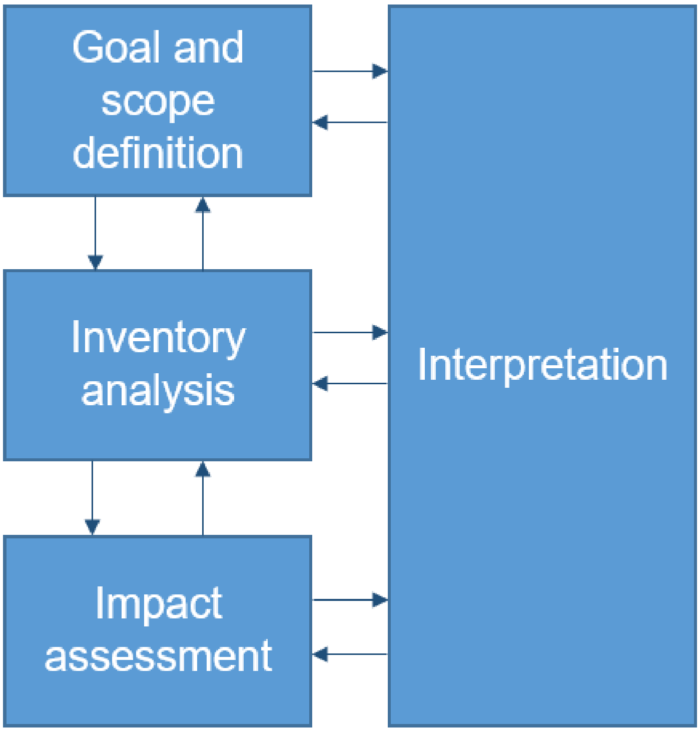

Figure 1 LCA framework adapted from [5].

The Ecoinvent database was used to associate the inputs into the supply chain with the chosen environmental inputs [7]. Missing datasets in the Ecoinvent databased, were supplemented by derivation according to previously published guidelines through substitution based on functional similarities or chemical characteristics [4, 8]. All materials were assumed to be virgin in nature.

A total of ten impacts were chosen to be compared in this study; global warming potential (GWP), acidification potential (AP), eutrophication potential (EP), freshwater aquatic ecotoxicity potential (FAETP), freshwater sediment ecotoxicity potential (FSETP), marine aquatic ecotoxicity potential (MAETP), marine sediment ecotoxicity potential (MSETP), human toxicity potential (HTP), land use and cumulative energy demand (CED). Each of these impact categories is explained further in Appendix 1.

The SCEnAT*i* (Supply Chain Environmental Analysis Tool- *intelligence*) decision support tool was used to provide the results of the hybrid LCA methodology. The tool allows additional supply chain inputs, that may not be accounted for by a process LCA methodology, to be captured and therefore provides a more representative result that a process LCA alone [9]. To complete this step, the following 'missing inputs' were applied to the system boundary of the chosen supply chain:

- Other general purpose machinery
- Recycling of metal waste and scrap
- Steam and hot water supply
- Telecommunications
- Computer services and related activities
- Research and development
- Collection of waste

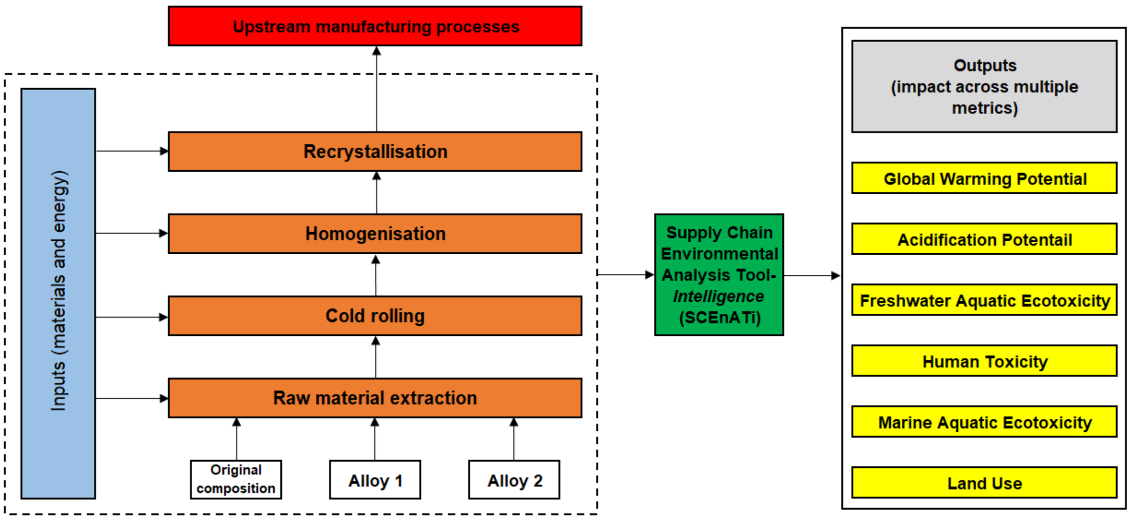

Figure 2 The system boundary of the magnesium alloy LCA; all process steps enclosed within the dotted lines are included in the LCA.

The LCC of the chosen supply chain is also developed by the SCEnAT*i* tool; no primary data was available to complete this step and therefore secondary costing data was taken from publically available data sources [10]. The methodology employed by SCEnAT*i* uses Multiregional Input Output (MRIO) tables to calculate the indirect cost analysis of the supply chain under investigation based on the missing inputs outlined above [9].

Finally, the SCEnAT*i* tool provides a supply chain carbon map to identify carbon hotspots and quantify their impacts (see Appendix 2).

3. Results

The hybrid LCA results are outlined below; a summary of the result for each alloy composition is shown. In addition to this composition level analysis, the electrical, thermal and material embedded energy distributions, the percentage contributions of each step within the system boundary to the GWP impact, the toxicological footprint of each material composition and the upstream greenhouse gas (GHG) emissions are provided.

Table 1 Summary of the hybrid LCA result for each alloy composition.

Alloy	Total GWP (kg CO_2-eq)	Total Cost (£)	Direct GWP (%)	Direct Cost (£)	Indirect GWP (%)	Indirect Cost (£)
Original composition	27.11	124.33	97.60	108.55	2.40	15.78
Alloy 1	27.11	124.45	97.60	108.66	2.40	15.79
Alloy 2	27.11	124.49	97.60	108.70	2.40	15.79

Table 1 shows that the GWP impact and direct-indirect contributions are not affected by the change in composition when the original steel composition is compared to the two new alloy types. Despite this, there is a small increase in cost per kg of material as the composition changes from the original composition to the new alloy configurations.

3.1. Composition level analysis

The percentage contributions of each alloying element within each alloy composition is shown in Figures 3-5.

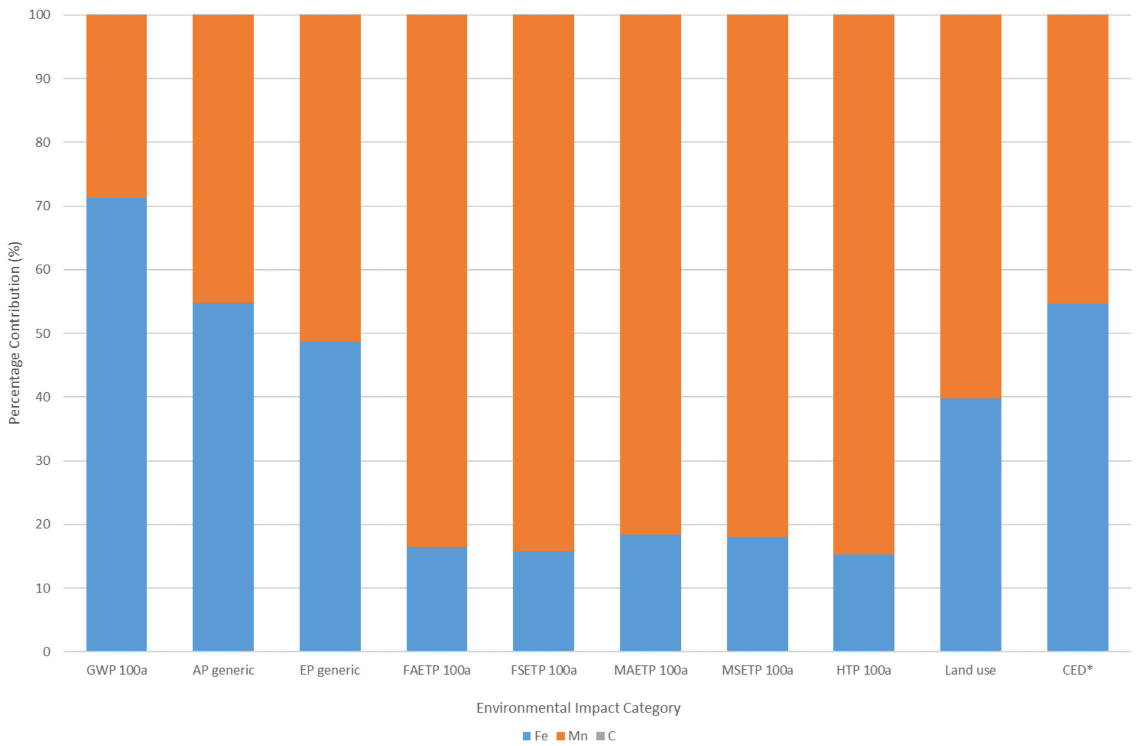

*Figure 3 Percentage contribution of each alloying material of the original alloy composition for the environmental impacts investigated. *Cumulative energy demand.*

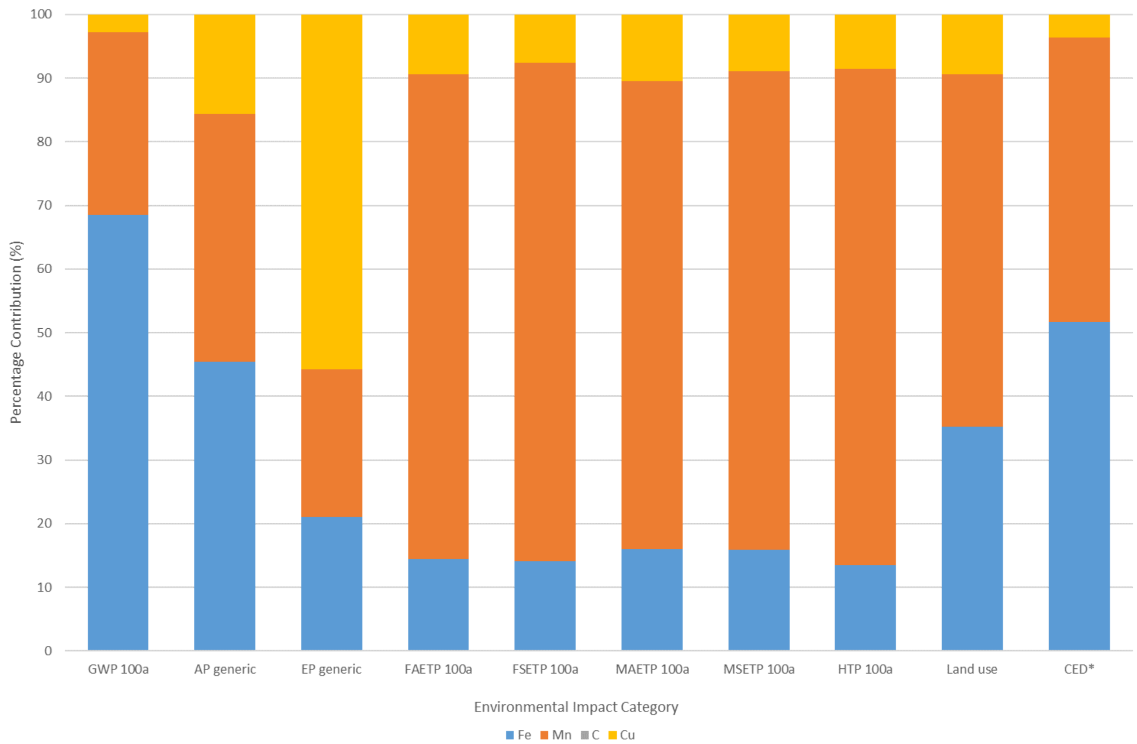

*Figure 4 Percentage contribution of each alloying material of Alloy 1 for the environmental impacts investigated. *Cumulative energy demand.*

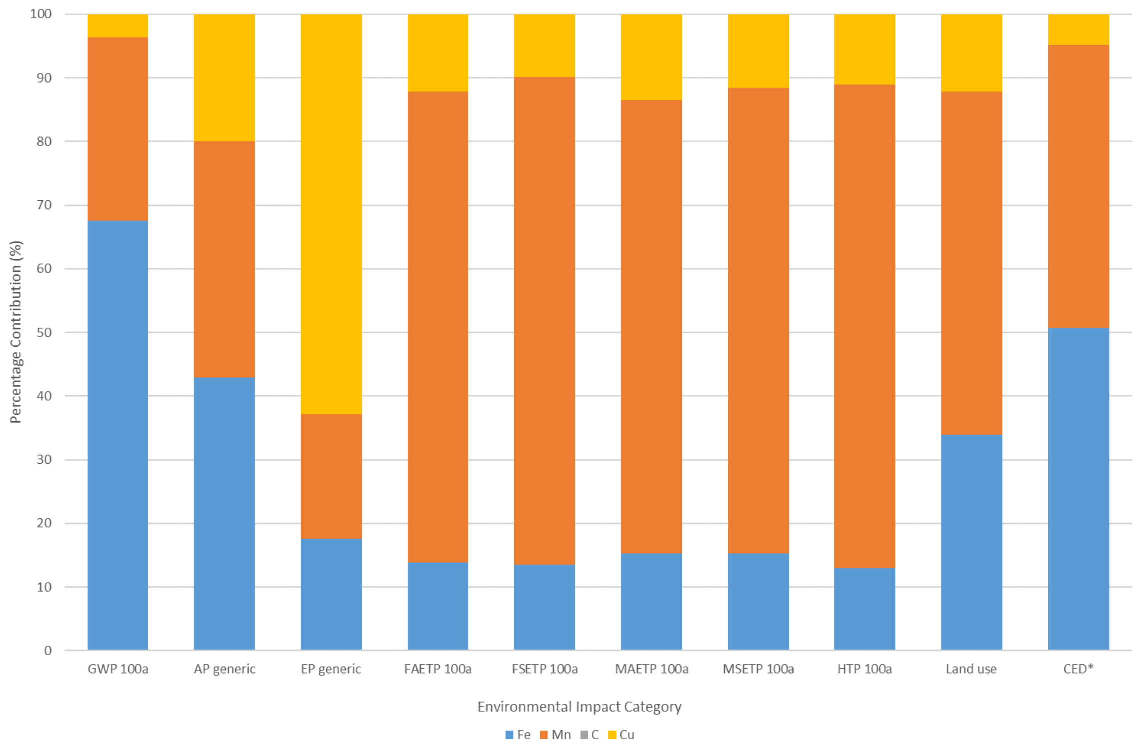

*Figure 5 Percentage contribution of each alloying material of Alloy 2 for the environmental impacts investigated. *Cumulative energy demand.*

The highest impact on the five toxicological impact categories (freshwater aquatic, freshwater sediment, marine aquatic and marine sediment ecotoxicity and human toxicity) is the use of manganese in the original alloy composition. Manganese also has a high impact on the eutrophication potential (originally alloy only) and land use impact categories; the use of copper in alloys 1 and 2 causes the highest eutrophication impact. It is the base element, iron, that causes the highest impact with respect to the global warming potential and the cumulative energy demand. This distribution is shown in Figure 3.

The change in alloy configurations from the original alloy to Alloy 1 and Alloy 2 requires the addition of copper (0.03 wt% and 0.04 wt% respectively). Figures 4 and 5 show that, the use of copper in the new alloy structures leads to a change in the distribution of the eutrophication potential impact. As with the original alloy composition, the use of manganese has a high impact on the toxicological impact categories, but iron still has the highest contribution to the global warming potential.

3.2. Energy distributions

The electrical, thermal and material embodied energies of the three alloy compositions are detailed in sections 3.2.1 to 3.2.3.

3.2.1. Electrical energy distribution

Figure 6 outlines the electrical energy distribution of the manufacturing processes required for all three alloy compositions. These processes were performed in the Materials Science and Engineering laboratory at the University of Sheffield. Although the power requirements relating to cold rolling are higher than those for the homogenisation and recrystallisation steps, the latter two processes take place over a longer period of time and therefore result in a higher electrical energy demand.

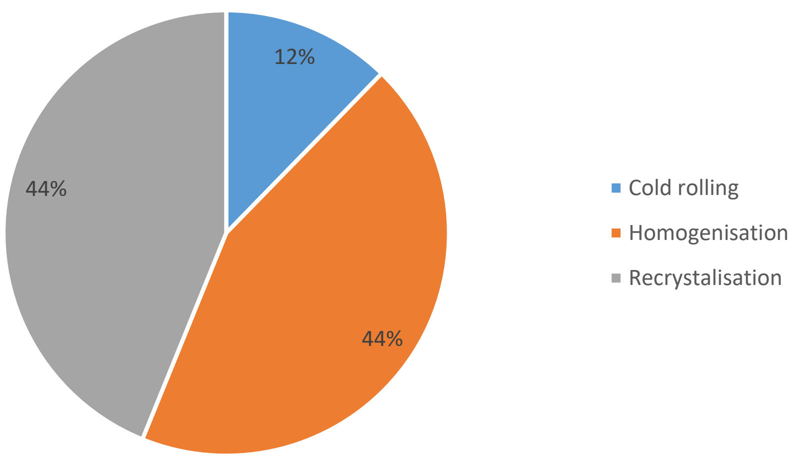

Figure 6 The percentage electrical energy contributions of each laboratory production process for all alloy compositions studied.

3.2.2. Thermal energy distribution

The thermal energy distribution of the three manufacturing processes required for all three of the alloy compositions studied are shown in Figure 7. The highest thermal energy demand is required by the homogenisation process; this is due to the high temperature requirements (1040°C) required to complete the process.

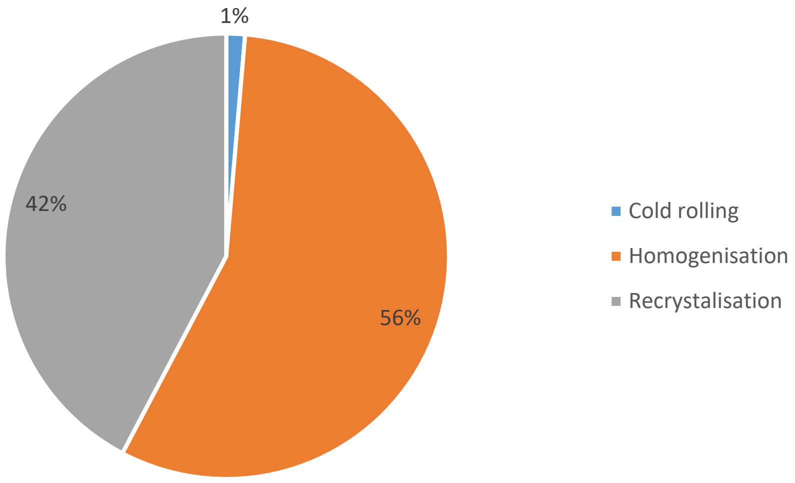

Figure 7 The percentage thermal energy contributions of each laboratory production process for all alloy compositions studied.

3.2.3. Material embedded energy distribution

The percentage contribution of the material embedded energy of each alloying element of the different alloy compositions are shown in Table 2. In each case, the high impact is from base element, iron which is closely followed by the impact of manganese.

Table 2 The percentage contribution of the material embedded energy of each alloying element within the alloy compositions studied.

Alloy	Total material embedded energy (MJ-eq)	Composition	% contribution of each alloying element
Original alloy	28.06	Fe	54.71
		Mn	45.28
		C	0.01
Alloy 1	28.50	Fe	51.76
		Mn	44.57
		C	0.01
		Cu	3.66
Alloy 2	28.65	Fe	50.8
		Mn	44.34
		C	0.01
		Cu	4.85

3.3 Material contribution to the global warming potential

The data shown in Table 3 breaks down the GWP impact of all the of the alloy compositions to show the percentage contribution to the impact caused by each material. Overall, when compared to the weight percentage, copper has the highest percentage impact to the alloy 1 and 2 compositions.

Table 3 Percentage contributions of each material input with respect to the GWP of the three alloy compositions studied.

	Original composition	**Alloy 1**	**Alloy 2**
	Total GWP impact (process LCA) (kgCO$_2$-eq)		
	2.0526	2.0518	2.0515
	% of GWP impact		
Iron	71.229	68.497	67.585
Manganese	28.764	28.775	28.779
Carbon	0.007	0.007	0.007
Copper	N/A	2.721	3.628

2.6 Toxicological impact of each alloy

The toxicological impacts of all four three compositions are shown in Figure 9. The composition of Alloy 2 leads to the highest toxicological impact, this result is broken down and analysed in more detail in section 3.5.

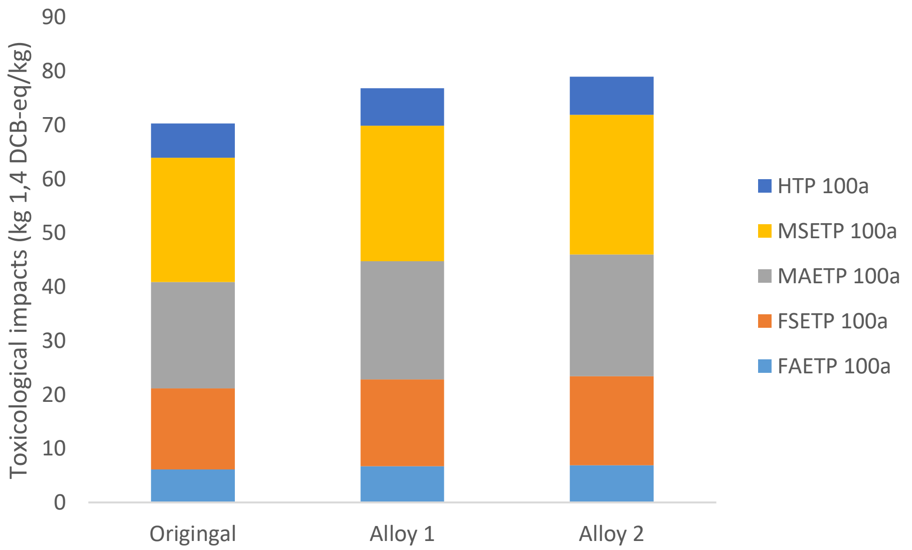

Figure 9 The total toxicological impact comparison for the original, Alloy 1 and Alloy 2 compositions. NB: human toxicity potential (HTP 100a), marine sediment ecotoxicity potential (MSETP 100a), marine aquatic ecotoxicity potential (MAETP 100a), freshwater sediment ecotoxicity potential (FSETP 100a) and freshwater aquatic ecotoxicity potential (FAETP 100a).

2.7 The upstream impact

Table 4 shows the distribution of the upstream IO GHG impact for each material composition, the three highest industries shown are utilities, mining and metals; “others” represents those industries with an impact lower than 0.01 kg CO_2-eq. It can be seen that there is very little difference between each impact when the different material configurations are compared, this is mirrored in the result provided in Table 1, though there is a small increase in the impact for the mining and business services input, highlighted in yellow.

Table 4 The upstream IO GHG emissions comparison for the original steel composition, alloy 1 and alloy 2. “Others” refers to those inputs with a carbon emissions contribution of less than 0.01 kg CO_2-eq.

Input	**Carbon emissions (kg CO_2-eq)**		
	Original alloy	**Alloy 1**	**Alloy 2**
Utilities	0.2955	0.2955	0.2955
Mining	0.1039	0.1040	0.1040
Metals	0.0635	0.0635	0.0635
Transport and communication	0.0398	0.0398	0.0398
Business services	0.0255	0.0256	0.0256
Minerals	0.0212	0.0212	0.0212
Chemicals	0.0174	0.0174	0.0174
Equipment	0.0151	0.0151	0.0151
Agriculture	0.0147	0.0147	0.0147
Fuels	0.0139	0.0139	0.0139
Other	0.0117	0.0117	0.0117

3. Discussion

3.1 Costings

Secondary data was used to determine the input costs of this supply chain within the system boundary, the individual costs of each element and energy source determined using up-to-date web sources, such as “Investmentmine” [10, 11]. In the event that primary data could be sourced from an industrial partner, the LCC portion of this study would be strengthened dramatically.

Table 1 outlines the total cost of each alloy, including the material and energy requirements. The cost is disaggregated to outline the direct costs and indirect costs. With respect to the direct costs, i.e. those concerning the materials and processes contained within the system boundary (Figure 2) for the functional unit of 1kg of material produced, the highest cost can be attributed to the electricity requirement at over 99% of the total cost. These costs would likely be reduced in an industrial setting due to process efficiency improvements when compared to laboratory based processes [4].

The hybrid LCA methodologies allows the indirect costs to be calculated using Multiregional Input-Output (MRIO) tables to calculate the additional costs to the supply chain which are not covered by the process methodology; overall, there is little change to the indirect costs of each alloy type, this can be attributed to the fact that the same industries are in play across the three supply chains studied [12].

3.2 Component level analysis

The process LCA provides the environmental impact of the material use within each steel composition, as shown in Table 3, this impact ranges from 2.0515 kg CO_2-eq for alloy 2 to 2.0526 kg CO_2-eq for the original steel composition. On comparison at this scale the range of results is small, this is due to the high proportion of iron used in each composition, despite this, the differences in the impacts of each material would become more important at higher production volumes.

The global warming potential (GWP) of iron can be attributed to the extraction phases required for metal extraction; it has been shown that, for iron ore specifically, its loading and hauling and crushing and screening requirements lead to the highest GWP impact. Furthermore, savings of 45.7% have been reported to be saved for loading and hauling when best available techniques are employed; this number increased to 157.4% for crushing and grinding [13].

The introduction of copper into alloy 1 and 2 clearly changes the distribution of the material contribution to the eutrophication potential, as shown in Figures 4 and 5. This is due to the release of SO_2, and other metals, related to the copper mining operation, which leads to the build-up nutrients in the ecosystem causing algae growth which reduces populations and water quality [14].

To achieve GWP savings for each of the steel compositions, focus should be made on implementing efficient mining techniques or exploiting recycled steels which have been shown to provide energy savings of 74% whilst reducing damage to local ecosystems [13].

3.3 Energy distribution

The electrical and thermal energy distributions are shown in Figures 6 and 7, as all three steel types undergo the same manufacturing processes, these figures represent all three alloys. The steel processing steps require cold rolling, homogenisation and recrystallisation, this requires a total of 37.63 kWh of electrical energy and 0.001 MJ of thermal energy. These figures are calculated using established methodologies [4].

While the watts associated with the cold rolling process are lower than those of the homogenisation and recrystallisation processes, the latter processes require twelve times the amount of processing time and therefore their final energy consumption is much higher. Furthermore, the homogenisation process is performed at 1040°C, compared to 780°C for the recrystallisation process and room temperature for the cold rolling process, therefore the homogenisation process requires the highest thermal energy demand.

The electrical and thermal energy requirements related to the production of these steel compositions would likely reduce in an industrial setting due to the use of processing parameters that are more efficient than in a laboratory [15]. While this assumption can be made, this report would be much more robust with the use of primary industry data.

3.4 Material embedded energy

The material embedded energy demand is also referred to as the cumulative energy demand (CED) which is calculated as the sum of the material energy demand of natural resources e.g. fossil, solar, nuclear, wind, primary forest, water and biomass) [4].

Although the use of iron in each alloy structure leads to the highest CED impact, as outlined in Table 2, the comparison of the wt% of manganese to the total CED impact is much higher than that of iron. It has been shown that the embodied energy of the metal extraction and refining processing of steel outweigh that of the mineral processing and concentration steps [13]. Furthermore, the amount of embodied energy increases as the ore grade decreases as an increase in material must be extracted; though this increase is not seen further down the supply chain as a fixed grade is manufactured for downstream processing which is not dependent on the original ire grade.

Overall, alloy 2 provides the highest material embodied energy impact; although manganese is not the highest contributor to the overall impact category, it has the highest wt% to impact ratio and therefore it would be necessary to concentrate efforts on reducing the manganese content to reduce the overall CED of the material.

3.5 Toxicology analysis

Each of the HTP, FAETP, FSETP, MAETP and MSETP impact categories are all measured in kg 1,4 DCB-eq and can therefore be aggregated and compared to provide further analysis of the material studied. Figure 9 shows that the alloy with the highest toxicological impact of the three compositions studied was alloy 2.

Although the highest wt% of material in all three cases is iron, it is the use of manganese that leads to the highest toxicological impact for each of the material compositions, this is shown in Figures 3-5. Overexposure to manganese, through industrial processes such as welding, has been found to lead to toxicity in the central nervous system, lungs and liver [16]. Manganese can also be considerably bioconcentrated in marine and freshwater environments, leading to increased temperatures and decreased pH for fish and invertebrates [17].

The introduction of copper to alloys 1 and 2 leads to a slight increase in each of the toxicological impact categories for these material compositions. The HTP is affected because the use of copper can cause issues such as liver toxicity [18] and increased levels of arsenic in the urine of those living close to copper smelters [19]. Heavy metal pollution of water courses, relating to the FAETP, FSETP, MAETP and MSETP impact categories, is a problem due to their non-biodegradable and accumulative characteristics; excessive concentrations of copper is toxic to other living creatures, especially fish [20].

If the toxicological footprints of these materials alone were taken into consideration, the original steel composition provides the lowest overall impact. Reduction of the manganese content in each steel structure would lead to the highest savings over the other alloying elements.

3.6 Upstream IO GHG emissions

Through the application of the hybrid LCA methodology, the system boundary of the process LCA is expanded to introduce impacts which may not be available to the modeller, thereby providing a more robust result than a process LCA alone [4]. For all three material compositions the three highest upstream impacts can be attributed to the utilities (47%), mining (17%) and metals (10%). Overall, the indirect impacts only lead to 2.4% of the overall GWP impact for each material composition and therefore little improvement to the total environmental impact could be made within the whole supply chain by targeting savings in these industries.

4. Limitations

The lack of primary, industry data is the main limitation to this study; current material and process costs, based on industry informed data would produce to a more robust result and therefore lead to more informed decision making. While process requirements relating to this study were calculated using established methods, as this study is based on laboratory scale manufacturing processes, it is likely to be an overestimate of the impact that would be seen in an industrial setting. Therefore, primary industrial energy usage data would again, provide a much more robust result to ensure informed decision making [4]. Similarly, informed industrial costing data would provide a more robust LCC and hybrid LCA result; the hybrid LCA result would be improved as this methodology relies on costing data to relate the environmental impacts to the MRIO tables [4].

There is a level of subjectivity provided by the choice of the additional inputs made by the modeller in the SCEnAT*i* decision support tool; this leads to a limitation in the final result as a second modeller may choose to impute different additional inputs. Despite this, the hybrid LCA methodology provided by the SCEnAT*i* decision support tool provides a more robust result when compared to the process LCA alone due to the expansion of the system boundary and therefore this potential effects of this subjectivity is outweighed by benefits provided by the methodology [21].

5. Conclusions

Taken alone, assessment of the GWP impact category of three steel compositions shows that the production of the original steel composition leads to the highest environmental impact, while alloy 2 has the lowest environmental impact. Taking other environmental impact categories into account, such as the toxicological footprint (comprising of the HTP, MAETP, MSETP, FAETP and MSETP impact categories) and the cumulative energy demand, shows that allow 2 has a higher environmental impact in these areas than the original steel composition. This provides a conundrum to the decision maker to decide which environmental impacts should take precedence in the final design.

Overall, the use of the hybrid LCA methodology to determine the environmental impacts of three steel compositions, designed for light weighting in the automotive industry, has provided a guide for the developers of the material to understand how the supply chain of that material affects the environment.

The use of iron and manganese in the structure lead to the main environmental impacts, although the small addition of copper to alloys 1 and 2 does not go unnoticed with regards to its toxicological impact.

The electrical energy requirement for manufacturing these steels leads to the carbon hot-spot within the supply chain and therefore, effort should be focussed into this area to provide the highest return on investment with regards to impact reduction. Despite this, this study uses laboratory manufacturing methods and therefore, in an industrial setting, these impacts are likely to be reduced due to processing efficiencies. Further, improvements to the environmental impact of these materials would be realised through the use of efficient mining processes and recycled materials.

While the substitution of materials to achieve environmental savings in the use phase of a product's life cycle is attractive, the environmental impacts of the substitutive materials must also be taken into account to ensure that further environmental damage is not sustained. The results of this study can provide the material designers with the tools to make these decisions.

References

[1] DARE. (06/03/2018). Available: http://darealloys.org/research-programme-overview/magnesium-alloys-that-are-less-dependent-on-rare-earths/

[2] Y. Wei, Y. Li, L. Zhu, Y. Liu, X. Lei, G. Wang*, et al.*, "Evading the strength–ductility trade-off dilemma in steel through gradient hierarchical nanotwins," *Nature Communications,* vol. 5, p. 3580, 04/01/online 2014.

[3] K. M. Rahman, V. A. Vorontsov, and D. Dye, "The effect of grain size on the twin initiation stress in a TWIP steel," *Acta Materialia,* vol. 89, pp. 247-257, 2015/05/01/ 2015.

[4] T. Ibn-Mohammed, L. S. C. Koh, I. M. Reaney, A. Acquaye, D. Wang, S. Taylor*, et al.*, "Integrated Hybrid Life Cycle Assessment and Supply Chain Environmental Profile Evaluations of Lead-based (Lead Zirconate Titanate) versus Lead-free (Potassium Sodium Niobate) Piezoelectric Ceramics," *Energy & Environmental Science,* vol. 9, pp. 3495-3520, 2016.

[5] International Organisation for Standardization, "ISO 14040:2006, "Environmental Management- Life cycle assessment- Principles and framework"," ed, 2006.

[6] A. Ahmed, I. Hassan, T. Ibn-Mohammed, H. Mostafa, I. M. Reaney, L. S. C. Koh*, et al.*, "Environmental life cycle assessment and techno-economic analysis of triboelectric nanogenerators," *Energy & Environmental Science,* vol. 10, pp. 653-671, 2017.

[7] Ecoinvent. (http://www.ecoinvent.org/ accessed 19/09/2017, 17th May 2018). Available: http://www.ecoinvent.org/

[8] G. Geisler, T. B. Hofstetter, and K. Hungerbühler, "Production of fine and speciality chemicals: procedure for the estimation of LCIs," *The International Journal of Life Cycle Assessment,* vol. 9, pp. 101-113, 2004.

[9] A. Lake, A. Acquaye, A. Genovese, N. Kumar, and S. C. L. Koh, "An application of hybrid life cycle assessment as a decision support framework for green supply chains," *International Journal of Production Research,* vol. 53, pp. 6495-6521, 2015.

[10] (June 2018). *Investment Mine*. Available: http://www.infomine.com/investment/

[11] J. H. Miah, S. C. L. Koh, and D. Stone, "A hybridised framework combining integrated methods for environmental Life Cycle Assessment and Life Cycle Costing," *Journal of Cleaner Production,* vol. 168, pp. 846-866, 2017.

[12] S. C. L. Koh, A. Genovese, A. A. Acquaye, P. Barratt, N. Rana, J. Kuylenstierna*, et al.*, "Decarbonising product supply chains: design and development of an integrated evidence-based decision support system – the supply chain environmental analysis tool (SCEnAT)," *International Journal of Production Research,* vol. 51, pp. 2092-2109, 2013.

[13] T. Norgate and N. Haque, "Energy and greenhouse gas impacts of mining and mineral processing operations," *Journal of Cleaner Production,* vol. 18, pp. 266-274, 2010.

[14] A. P. Acero, C. Rodriguez, and A. Ciroth. (29th May 2018). *Green Delta*. Available: http://www.openlca.org/wp-content/uploads/2016/08/LCIA-METHODS-v.1.5.5.pdf

[15] H. Walker, L. Di Sisto, and D. McBain, "Drivers and barriers to environmental supply chain management practices: lessons from the public and private sectors," *Journal of Purchasing and Supply Management,* vol. 14, pp. 69-85, 2008.

[16] J. Crossgrove and W. Zheng, "Manganese toxicity upon overexposure," *NMR in Biomedicine,* vol. 17, pp. 544-553, 2004.

[17] P. Howe, H. Malcolm, and S. Dobson, *Manganese and its compounds: environmental aspects*: World Health Organization, 2004.

[18] P. G. Georgopoulos, S. W. Wang, I. G. Georgopoulos, M. J. Yonone-Lioy, and P. J. Lioy, "Assessment of human exposure to copper: A case study using the NHEXAS

database," *Journal Of Exposure Science And Environmental Epidemiology,* vol. 16, p. 397, 10/26/online 2005.

[19] L. Polissar, K. Lowry-Coble, D. A. Kalman, J. P. Hughes, G. van Belle, D. S. Covert*, et al.*, "Pathways of human exposure to arsenic in a community surrounding a copper smelter," *Environmental Research,* vol. 53, pp. 29-47, 1990/10/01/ 1990.

[20] L. Deng, Y. Su, H. Su, X. Wang, and X. Zhu, "Biosorption of copper (II) and lead (II) from aqueous solutions by nonliving green algae Cladophora fascicularis: Equilibrium, kinetics and environmental effects," *Adsorption,* vol. 12, pp. 267-277, July 01 2006.

[21] L. Smith, T. Ibn-Mohammed, F. Yang, I. Reaney, D. C. Sinclair, and S. C. L. Koh, "Comparative Environmental Profile Assessments of Commercial and Novel Material Structures for Solid Oxide Fuel Cells," *Applied Energy,* vol. 235, pp. 1300-1313, 2019.

Appendix 1

A total of ten impacts were chosen to be compared in this study; global warming potential (GWP), acidification potential (AP), eutrophication potential (ET), freshwater aquatic ecotoxicity potential (FAETP), freshwater sediment ecotoxicity potential (FSETP), marine aquatic ecotoxicity potential (MAETP), marine sediment ecotoxicity potential (MSETP), human toxicity potential (HTP), land use and cumulative energy demand (CED). Each of these impact categories is explained in more detail below.

The GWP, given as kg CO_2-eq, is a calculates climate change and is based on the UN's Intergovernmental Panel on Climate Change (IPPC) factors with a time horizon of 100 years (other time horizons can also be assessed but this is the most common). Factors taken into consideration are the effect of greenhouse gases on biodiversity, climate phenomenon and temperature [14].

AP, expressed as kg SO_2-eq, is a measure of acidification due to the release of SO_2 and NO_x into the atmosphere leading to acid rain. Acidification leads to a reduction in biodiversity and damage to the ecosystem, this usually takes place in foreign regions to the initial gas release [14].

When nutrients build up in ecosystems due to the release of ammonia, NOx, nitrates and phosphorus in the air and water, this is called eutrophication which leads to adverse effects such as the growth of algae which reduces populations and water quality. The EP measures this change as either kg PO_4^{3}-eq or kg N-eq, depending on the reference model [14].

The FAETP, FSETP, MAETP and MSETP address the impact of toxic substances in each of the associated ecosystems. The maximum tolerable concentration of materials, such as heavy metals, in water for ecosystems is calculated using the European Union's toxicity model and is expressed as kg 1,4-DB-eq [14].

Human toxicity is measured by the HTP, which is calculated based on the toxicity of a compound and its potential does, the units used at kg 1,4-DB-eq. The aim of the impact category is to determine the harm of a chemical when it is released to the environment. The indicators used are cancer, respiratory diseases, non-carcinogenic effects and effects to ionising radiation.

The consumption of a material, based on natural resources such as fossil, nuclear, solar and wind defines the CED, this is also known as the material embedded energy and is expressed as MJ-eq [4].

Appendix 2

This section provides the supply chain carbon maps produced by the SCEnATi decision support tool for each of the three steel compositions. The output is colour coordinated; a red box represents a very high impact, above 10%; high impact (5-10%) is shown in orange; medium impact (1-5%) is given in yellow; low impact (less than 1%) is depicted in green.

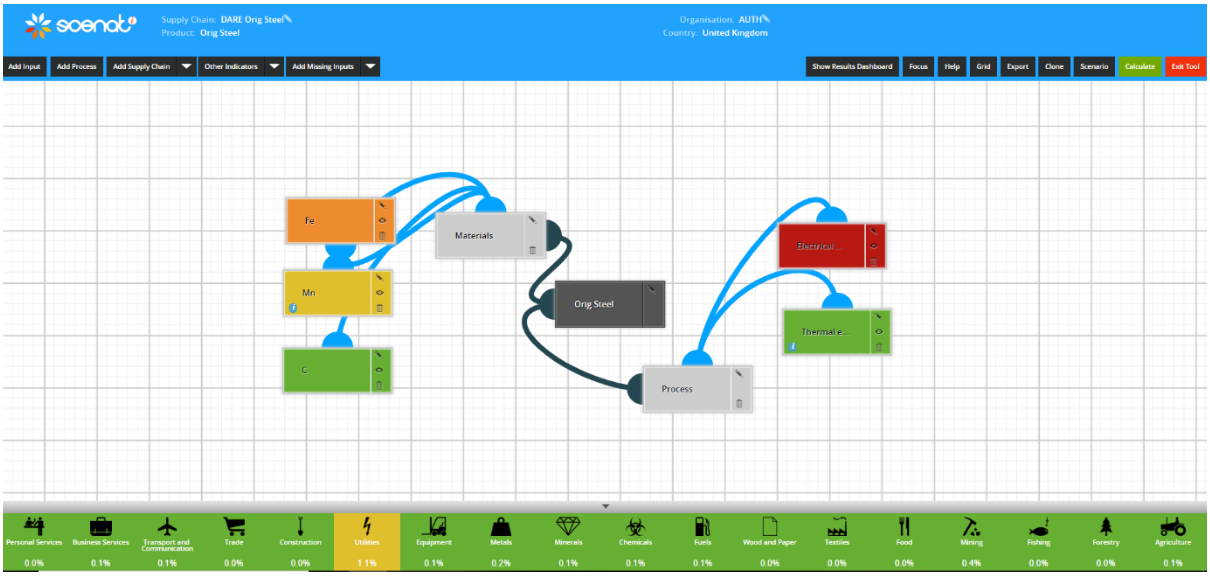

Figure A2-1 SCEnATi supply chain carbon map for the original steel composition

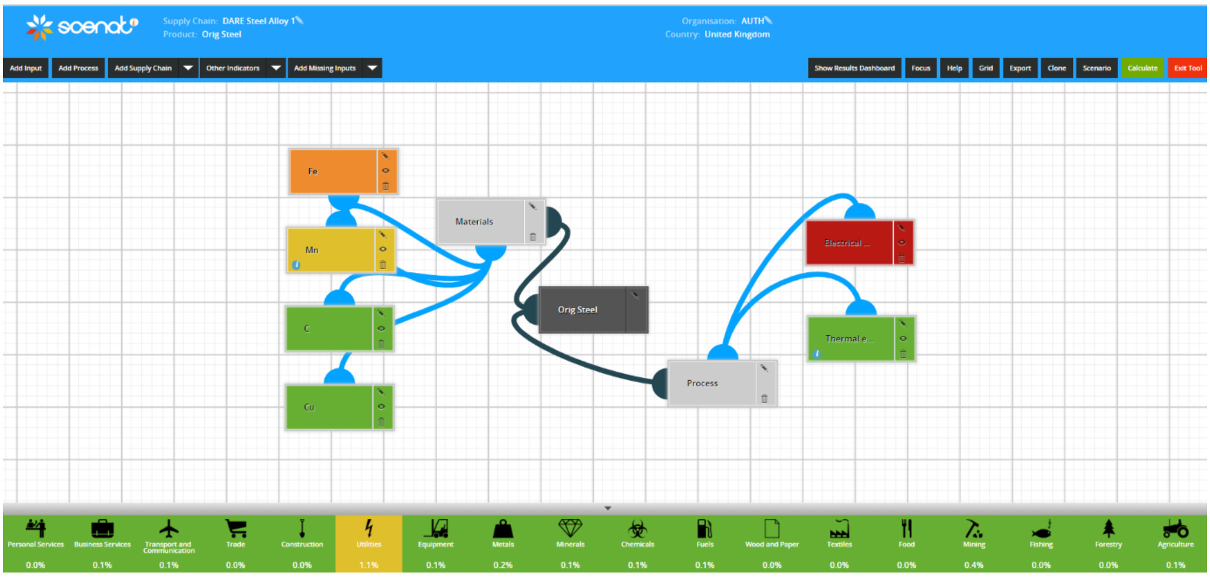

Figure A2-2 SCEnATi supply chain carbon map for Alloy 1

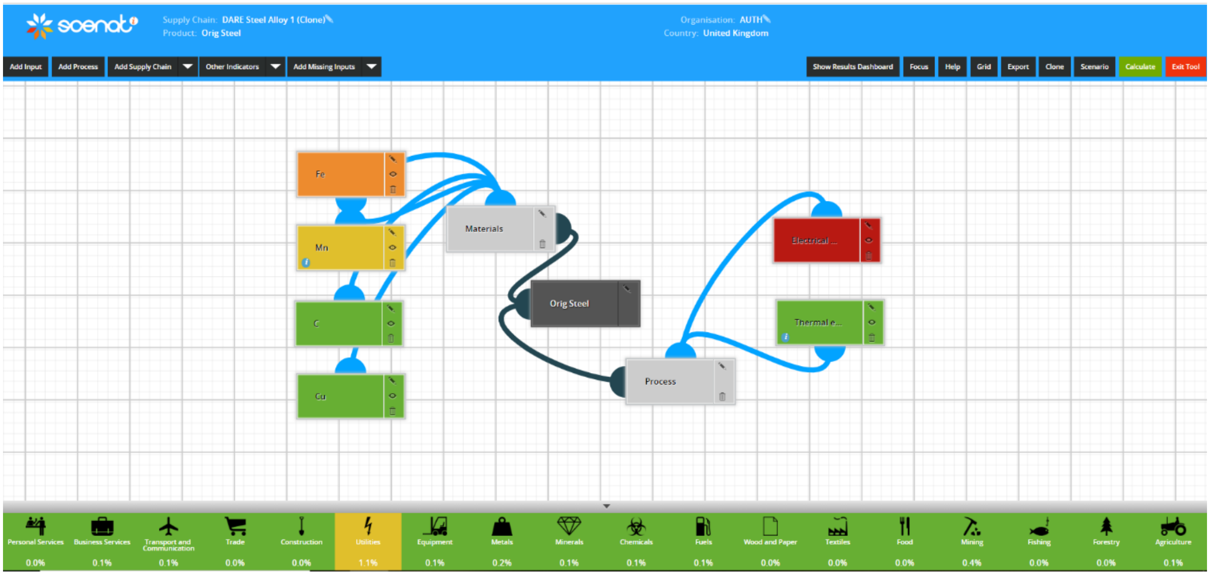

Figure A2-3 SCEnATi supply chain carbon map for Alloy 2

Appendix 3

This section provides a breakdown of the Life Cycle Inventories for each of the alloy compositions studied.

Table A3-1 LCI of the original steel composition

Alloy component	**kg/kg**	**Ecoinvent reference**
Fe	0.774	cast iron production, cast iron [kg] RER 35% scrap, 65% pig iron assumed iron input
Mn	0.22	manganese production, manganese [kg] RER
C	0.006	graphite production, graphite [kg] RER

Table A3-2 LCI of Alloy 1

Alloy component	**kg/kg**	**Ecoinvent reference**
Fe	0.744	cast iron production, cast iron [kg] RER 35% scrap, 65% pig iron assumed iron input
Mn	0.22	manganese production, manganese [kg] RER
C	0.006	graphite production, graphite [kg] RER
Cu	0.03	copper production, primary, copper [kg] RER

Table A3-3 LCI of Alloy 2

Alloy component	**kg/kg**	**Ecoinvent reference**
Fe	0.734	cast iron production, cast iron [kg] RER 35% scrap, 65% pig iron assumed iron input
Mn	0.22	manganese production, manganese [kg] RER
C	0.006	graphite production, graphite [kg] RER
Cu	0.04	copper production, primary, copper [kg] RER